Accepted version of paper presented in poster form at OCEANS'11 MTS/IEEE Kona, Hawaii, 2011

The Importance of Mooring Line Model Fidelity in Floating Wind Turbine Simulations

Matthew Hall*, Brad Buckham*, Curran Crawford*, and Ryan S. Nicoll†

*Department of Mechanical Engineering, University of Victoria
Victoria, British Columbia, Canada

†Dynamic Systems Analysis Ltd.
Victoria, Britich Columbia, Canada

***Abstract*—Accurate computer modelling is critical in achieving cost effective floating offshore wind turbine designs. In floating wind turbine simulation codes, mooring line models often employ a quasi-static approximation that neglects mooring line inertia and hydrodynamics. The loss of accuracy from using this approach has not been thoroughly quantified. To test whether this widely-used simplified mooring line modelling approach is adequate, the open-source floating wind turbine simulator FAST was modified to allow the use of an alternative, fully dynamic, mooring model based on the hydrodynamics simulator ProteusDS.**

The OC3-Hywind floating wind turbine design was implemented in this newly-coupled simulator arrangement and tested using a variety of regular wave conditions. The static equivalence between the built-in quasi-static mooring model and the newly-coupled dynamic mooring model is very good. Tests using both models were performed looking at scenarios of the response of the system in still water and the response to regular waves and steady winds. The dynamic mooring model significantly increased the overall platform damping in translational DOFs during motion decay tests in still water. There was very little difference between the models in coupled tests where regular wave excitation was the primary driver of platform motions, except for the addition of small levels of power in the higher frequencies of the platform motion spectrum. The nature of the different tests suggests that it is only in situations where the platform motions and wave velocities are not synchronized that the damping from the dynamic mooring model makes a large difference. This points to irregular wave conditions as providing a better test of the differences between mooring models.

I. Introduction

Floating wind turbines offer a means to vastly expand the population of possible sites for offshore wind energy plants. By using a floating support platform secured by mooring lines, a wind turbine can be installed in waters exceeding the 30 m depth that limits conventional bottom-fixed offshore wind turbines [1]. This is of particular value for countries like Canada and the United States where suitably-shallow offshore sites are limited. The floating wind turbine industry is still in its infancy, with a wide range of designs proposed but only one MW-scale prototype, the Hywind, built to date, hence accurate models will be required to identify the most promising design approaches.

With the added degrees of freedom and loads that come from a floating support platform and its mooring lines, the dynamics of floating wind turbines are considerably more complex than those of bottom-fixed wind turbines. This poses challenges for both the platform and mooring system design and the simulation codes used to model the combined system. With the cost-sensitive nature of offshore wind energy, any overdesign required to compensate for uncertainties in the modelling techniques used can be a serious roadblock. As modelling accuracy is improved and verified, more cost-effective designs can be engineered and design concepts can be more accurately compared against each other to determine with confidence which configurations are the most promising.

A wide variety of platform and mooring concepts exist for floating wind turbines. They can most easily be classified by stability class - how they achieve hydrostatic stability. Ballast stabilized designs, such as the Hywind, use ballast to lower the center of gravity below the center of buoyancy and tend to be of the spar-buoy configuration. Buoyancy stabilized designs use a wide water plane area to raise the height of the metacenter above the center of gravity and are commonly of the barge or tri-floater (three vertical cylinders) configurations. Mooring stabilized designs, also known as tension leg platforms (TLPs), use well-spaced vertical mooring lines under significant tension against the floater buoyancy to submerge and stabilize a very buoyant platform.

Each of these classes has different platform hydrodynamics and mooring system characteristics. Ballast-stabilized designs tend to have very large natural periods and move minimally in typical waves, but need to operate at a small non-zero pitch angle to counter the wind turbine thrust moment. Their mooring lines, connected close to the center of gravity, tend to have a slack catenary profile due to a large line length to depth ratio. Dynamic mooring loads are relatively small for this stability class.

Buoyancy-stabilized designs tend to be more susceptible to wave-induced motion but more stiff when it comes to resisting pitching moments from static thrust. They also tend to use slack catenary mooring lines that, with the wide platform, tend to be connected further from the center of gravity. These factors combine to make for relatively large mooring line motions. Hence, dynamic mooring effects are relatively important for this stability class.

Mooring-stabilized designs tend to have platforms that are mostly submerged, making for minimal wave-induced

motions. Their taught, usually-vertical mooring configuration makes them extremely stiff in heave, roll, and pitch DOFs, but less stiff than other configurations in surge, sway, and yaw DOFs. The high line tensions also make these designs subject to high-frequency ringing forces in the lines.

Popular floating wind turbine simulators currently tend to use quasi-static mooring models in the form of either force-displacement relationships or analytical solutions for catenary cables in static equilibrium [2]. These approaches have the advantage of computational efficiency, which is desirable since the rest of the floating wind turbine model (aero-servo-elastic) tends to run quite quickly. For cases where waves are small and thus support platform and mooring line motions are minimal, quasi-static models provide a good approximation to reality. For cases with higher platform and mooring line motions, quasi-static mooring models neglect dynamic effects that may be significant. Often, the primary effect of the mooring line dynamics on the overall system is to increase the damping on the platform to the benefit of platform stability. For that reason, it has been argued that using a quasi-static model under-predicts the stabilizing effect of the mooring lines and is therefore a conservative modelling approach [3].

At the same time, the conservative approach of neglecting the damping from the line dynamics has drawbacks; for unmanned offshore wind turbines, where the safety factors are lower and cost margins slimmer than other offshore structures, under-predicting the damping on the platform may result in overdesign that compromises competitiveness. Additionally, in some cases the mooring line dynamics that quasi-static models neglect can be sources of increased structural loading on the turbine - through effects such as snap loads during extreme events or ringing from high line tensions.

What is missing is the literature is an evaluation of how important the dynamic effects of the mooring lines are for a given system. Cordle identified the need for a dedicated study into the importance of dynamic mooring line effects for floating wind turbines, and how different water depths and system designs impact the dynamic effects [2]. Two recent studies make steps in that direction. Waris and Ishihara [4] compared coupled simulation results of a tri-floater design using a linear force-displacement mooring model and a fully dynamic finite element mooring model, as well as experimental results. Their study identified important limitations to linear force-displacement models but did not compare dynamic and nonlinear quasi-static models. A study by Kallesoe and Hansen [5], used the simulation code HAWC2 with the addition of an FEM-based dynamic mooring model. The original, quasi-static mooring model in HAWC2 uses lookup tables describing the nonlinear force-displacement relationships of the mooring system. The study analyzed the dynamics of the OC3 Hywind system under a number of normal operation conditions, and concluded that the dynamic mooring model showed similar extreme loads but reduced fatigue loads compared to the original quasi-static model.

The current work focuses on the fully-coupled floating wind turbine simulation code FAST. FAST features a quasi-static mooring model that solves a set of analytical catenary cable equations to determine the instantaneous static-equilibrium positions and tensions of the mooring lines. This quasi-static model is compared with a fully-dynamic FEM-based mooring model, ProteusDS, that has been coupled with the FAST simulator. FAST remains in charge of the floating platform hydrodynamics modelling in both cases. The OC3-Hywind, a spar-buoy design with three catenary mooring lines, is the design chosen for the comparison effort because of its well-studied characteristics. Simulations have been done using steady winds and still or regular wave conditions. Simulating identical scenarios with both the quasi-static and the dynamic mooring models allows detailed evaluation of the impact of the mooring line dynamics on the overall simulation.

The paper is structured as follows. Section II discusses the simulation tools used and how they were coupled, the details of the OC3-Hywind design, and the test cases that were simulated. Section III presents the results of the comparison effort, showing the static equivalence of the two mooring models, and how they differ in damping the platform motions and affecting the response of the system under various conditions. Section IV reiterates the main findings from the results section and concludes.

II. Methodology

A. Coupled Simulator

The main software for this modelling effort is FAST, a fully coupled aero-hydro-servo-elastic time domain simulator for horizontal axis wind turbines. It is distributed by NREL. It combines limited structural degrees of freedom with Blade-Element-Momentum (BEM) aerodynamics, linear hydrodynamics for the floating platform, and a quasi-static treatment of the mooring line behavior. It interfaces with the open source BEM-based aerodynamics model AeroDyn. It uses mode shapes for its structural model. The entire formulation of the tower and turbine assumes small tilt angles of the platform and tower base. The platform hydrodynamics for the simulation of floating wind turbines are handled by HydroDyn, a linear hydrodynamics model that uses frequency domain data from the linear hydrodynamics preprocessor WAMIT to model the hydrodynamic loads on the floating platform [3].

FAST treats the floating platform as a rigid body and handles it separately from the elastic elements of the system - the tower, shaft, and rotor. FAST sends the position and velocity of the tower base to HydroDyn, the floating platform module, which then returns the forces and moments from the platform (including mooring line loads) to be applied at the base of the tower. The hydrodynamic loads on the platform are composed of three components from linear hydrodynamic theory - hydrostatic restoring, wave excitation, and wave radiation forces - and the drag term from Morison's equation. This drag term augments the linear hydrodynamics with a quadratic drag force, calculated using strip theory and the "'effective diameter"' of the platform [3].

FAST's quasi-static mooring line subroutine, Catenary, models the individual taut or slack catenary mooring lines. It

accounts for weight and buoyancy, axial stiffness, and friction from variable contact on the seabed, but does not account for bending or torsional stiffnesses. Being quasi-static, it solves for cable positions and tensions under static equilibrium given the instantaneous fairlead (cable-platform connection) location. Cable inertia and hydrodynamic forces are ignored [3].

This makes each mooring line lie in a catenary shape along a vertical plane whose corners are defined by the fairlead and anchor locations. With this simplification, the horizontal and vertical tensions at the fairlead can then be solved for by the numerical solution of two analytical equations of those two unknowns. If there is no seabed contact (the angle of the line at the anchor is greater than zero), then the following equations are used.

$$x_F(H_F,V_F)=\frac{H_F}{\omega}\left\{\ln\left[\frac{V_F}{H_F}+\sqrt{1+\left(\frac{V_F}{H_F}\right)^2}\right]-\ln\left[\frac{V_F-\omega L}{H_F}+\sqrt{1+\left(\frac{V_F-\omega L}{H_F}\right)^2}\right]\right\}+\frac{H_F L}{EA} \quad (1)$$

$$z_F(H_F,V_F)=\frac{H_F}{\omega}\left[\sqrt{1+\left(\frac{V_F}{H_F}\right)^2}-\sqrt{1+\left(\frac{V_F-\omega L}{H_F}\right)^2}\right]+\frac{1}{EA}\left(V_F L-\frac{\omega L^2}{2}\right) \quad (2)$$

In these equations, x_F and z_F are the horizontal and vertical fairlead coordinates, H_F and V_F are the horizontal and vertical components of the line tension at the fairlead, ω is the line weight per unit length, L is the unstretched line length, and EA is the axial stiffness of the mooring line. A modified set of equations is used when part of the cable length is in contact with the sea floor.

These equations provide the forces from the mooring lines. FAST uses additional analytic equations to specify the positions and tensions along the length of each line.

B. Dynamic Mooring Model

ProteusDS is a time domain hydrodynamics simulator developed by Dynamic Systems Analysis Ltd. and researchers at the University of Victoria that specializes in underwater cable and net dynamics. It can simulate floating systems composed of both rigid structures and flexible cables and nets. It features a fully dynamic nonlinear cable model, based on the work of Buckham et al. [6]. This model includes the effects of the distributed hydrodynamic loading on the cable as well as friction and normal elasticity and damping from cable contact with the seabed. The continuous equation of motion at any point on a mooring cable is [6]:

$$-(EI\mathbf{r}'')''+[((EA\varepsilon+C_{ID}\dot{\varepsilon})-EI\kappa^2)\mathbf{r}']+[GJ\tau(\mathbf{r}'\times\mathbf{r}'')]'+\mathbf{h}+\mathbf{w}=\mathbf{M}_I\ddot{\mathbf{r}} \quad (3)$$

where $\mathbf{r}(s,t)$ is the absolute position of the cable centerline with components defined relative to an inertial reference frame, $\mathbf{h}$ is the hydrodynamic load per unit length, $\mathbf{w}$ is the apparent weight of the cable per unit length, $\mathbf{M}_I$ is a 3 by 3 mass matrix (specific to the inertial frame axes) that includes direction-dependant added mass terms, and C_{ID} is an internal damping coefficient. Variables ε, κ, and τ are the axial strain, curvature, and twist, respectively, and EA, EI, and GJ are the respective stiffnesses of the cable for each type of deformation.

ProteusDS uses a finite element discretization of (3) with the cable mass lumped at the node points. The state of a simulated cable is defined by a twisted spline approximation to the cable centerline, $\mathbf{r}(s,t)$, plus a linear approximation to the twist, τ, of the cable cross section about the centerline. The state variables used in these two polynomial approximations are absolute positions, curvatures, and a single rotation angle, measured about the tangent direction, at each of the model node points. By expressing the cable dynamics in terms of absolute coordinates, the model is a form of the Absolute Nodal Coordinate Formulation (ANCF) presented by Berzeri and Shabana [7].

The twisted spline approximation ensures second order continuity between elements, but to ensure smoothness in the assembly boundary conditions must be applied between elements. These additional constraint equations allow the curvatures to be recovered at any time from the assembled set of node positions. Thus, for an assembled cable, the curvatures can be eliminated from the discretized equations. The cable twist model is composed of a torsion calculated from the approximated centerline and a rotation of the cross section about the tangent. Thus, given a set of node positions and a series of cross section rotations, the axial, bending, and torsional strains experience in the cable can be calculated. Equation (3) is used to explicitly solve for node accelerations that are integrated to determine the complete cable configuration at the next time step [6].

The hydrodynamic forces are calculated using Morison's equation. The added mass contribution, a function of the cable volume, orientation, water density, and an added mass coefficient, C_a, is included in $\mathbf{M}_I$. The drag term, $\mathbf{h}$ in (3), is calculated as:

$$\mathbf{h}=-\frac{1}{2}\rho_W d_C \mathbf{R}_{IH}\begin{bmatrix} f_p C_D \frac{-v_{p1}}{\sqrt{v_{p1}^2+v_{p2}^2}}|\mathbf{v}|^2 \\ f_p C_D \frac{-v_{p2}}{\sqrt{v_{p1}^2+v_{p2}^2}}|\mathbf{v}|^2 \\ -f_q C_D \operatorname{sgn}(v_q)|\mathbf{v}|^2 \end{bmatrix} \quad (4)$$

where $\mathbf{R}_{IH}$ is a rotation matrix from a reference frame attached and oriented with the cable (used solely for evaluating the hydrodynamics) to the inertial reference frame, d_c is cable diameter, v_x, v_y, v_z are the components of the relative velocity of the cable through water, C_D is a normal drag coefficient, and f_p and f_q are non-linear loading coefficients that determine the distribution of the scaled drag force between the normal and tangential directions of the local hydrodynamic frame based on the relative orientation of the cable centerline

and the relative velocity vector. The cable's relative velocity is given by $\mathbf{v}$:

$$\mathbf{v} = \dot{\mathbf{r}} - \mathbf{j} \tag{5}$$

where $\mathbf{j}$ is the water's absolute velocity at the point considered. When expressed in the local frame, the components of $\mathbf{v}$ are v_{p1}, v_{p2} and v_q where $p1$, $p2$ and q are the normal, binormal and tangent directions of the local hydrodynamic frame.

The ProteusDS cable model is also available in dynamic link library (DLL) form, which enables coupling to aerodynamic or aero-servo-elastic wind turbine codes for fully coupled floating wind turbine simulation making use of ProteusDS's dynamic cable model.

C. FAST-ProteusDS Coupling

The two simulators are arranged so that FAST transmits fairlead locations and velocities to ProteusDS, and ProteusDS in turn provides the line tensions/forces at the fairleads to FAST. This coupling is performed at every FAST time step. With its FEM implementation, the ProteusDS model requires a much smaller internal time step - approximately one-tenth the FAST time step. Matching between the two different time steps is handled internally by the ProteusDS DLL. Matching of regular wave kinematics between the two models has also been accomplished. A technique for matching irregular wave kinematics have not yet been developed and so the current work is limited to testing under regular wave forcing.

To couple ProteusDS into the platform dynamics subroutine of FAST (HydroDyn), a number of changes were made to the FAST source code, including the addition of a new subroutine that interacts with the ProteusDS DLL in place of the default quasi-static mooring subroutine, and modifications to the FAST input and output variables relating to the mooring system. In addition, an intermediate DLL was created to provide data type conversion between FAST and ProteusDS and to load and store information about the mooring system needed for initial condition generation and mooring fairlead position and force calculations.

D. Turbine System Description

The floating wind turbine design selected for this first comparison with the newly-coupled dynamic mooring model is the OC3-Hywind. The OC3-Hywind is based on the Statoil Hywind prototype that is the world's first MW-scale floating wind turbine, but modified for the purposes of the Offshore Code Comparison Collaboration (OC3) project, an international effort to compare and validate leading floating wind turbine simulation codes [8]. The OC3-Hywind design was used to compare simulators in terms of aerodynamic, structural, and especially hydrodynamic models in the OC3 Phase IV study.

The Hywind is a spar-buoy design with three slack catenary mooring lines. A graphic of the OC3-Hywind system is shown in Fig. 1. The OC3-Hywind design makes use of the NREL 5MW offshore reference wind turbine, a hypothetical design with standardized specifications to enable accurate comparison

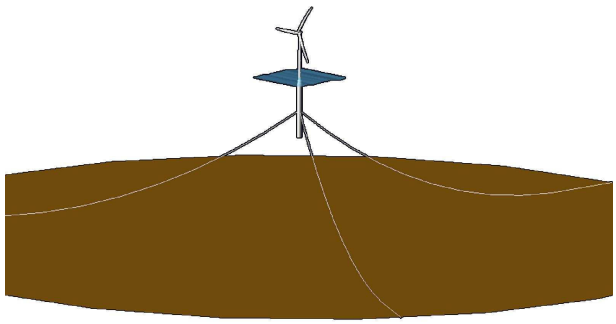

Fig. 1. OC3-Hywind system. Taken from [9].

of different wind turbine modelling tools. It also has a simplified mooring system, which simplifies the present comparison effort. The ballast-stabilized configuration results in minimal wave-induced motions and less mooring line dynamics than designs from other stability classes. However, the availability of information on its characteristics and specifications makes it a good design to start with in comparing different mooring models.

The OC3 Hywind specifications as set for the OC3 project were used in the current work [9]. FAST input files for the design were available from NWTC. Selected properties of the design are listed in Table I.

TABLE I
SELECTED OC3-HYWIND SPECIFICATIONS [9]

Tower top height above SWL	87.6 m
Tower mass	249718 kg
Platform draft	120 m
Platform mass	7466330 kg
Platform diameter above taper	6.5 m
Platform diameter below taper	9.4 m
Taper depth below SWL	4-12 m
Number of mooring lines	3
Water depth	320 m
Fairlead depth	70 m
Fairlead radius from centerline	5.2 m
Anchor radius from centerline	853.87 m
Mooring line unstretched length	902.2 m
Mooring line diameter	0.09 m
Mooring line mass density	77.7 kg/m
Mooring line EA	384243 kN
Mooring line EI	38 kN-m^2
Mooring line GJ	38 kN-m^2

Several details about the implementation of the design are worth noting. The definition of the OC3-Hywind includes the specification of additional hydrodynamic damping terms in surge, sway, heave, and yaw in order to provide for realistic damping levels that are not fully captured by the linear hydrodynamics preprocessing in WAMIT. These are included in the present model.

The OC3-Hywind design has a tapered (non-constant) diameter over part of its draft. Because viscous drag effects are significant for a spar-buoy, the viscous drag calculations in FAST were altered for the OC3 studies to account for this

changing diameter. This was done here as well.

In creating the mooring line input files for the ProteusDS model, bending and torsional stiffnesses (which are not included in the OC3 specifications) were estimated by scaling ratios of axial and bending/torsional stiffness taken from published wire rope test results. This approach is quite crude, but tests have shown very little sensitivity to large changes in the cable bending stiffness.

E. Test Cases

The comparison of the dynamic and quasi-static mooring models was completed using a selection of test scenarios taken from the OC3 phase IV study. These tests follow the numbering scheme of the OC3. Two additional test scenarios, which tested the sensitivity of the ProteusDS model to the number of cable elements and the static equivalence of the two mooring models, were completed. In all cases the wind and wave directions are coincident, in the positive x direction.

The test cases looked at in the current study include:

- Load Case 1.4 tests the unforced transient response of each DOF of the platform. The mass of the entire system is included but only the hydrodynamic and mooring line forces are enabled - aerodynamic forces are disabled. The six tests in this load case each start with the platform displaced from equilibrium along one of it's DOFs, with still water conditions, and the return to equilibrium is simulated.
- Load Case 4.1 tests the steady state response of the system to regular waves of 6 m height and 10 s period. Aerodynamic forces are disabled
- Load Case 5.1 tests the steady state response of the system to steady, uniform 8 m/s winds as well as regular waves of 6 m height and 10 s period.
- Load Case 5.4 tests the steady state response of the system to steady 8 m/s winds and unit-amplitude (2 m height) regular waves of varying frequency. This allows computation of response amplitude operators (RAOs) that define the amplitude of response of various system motions and forces per unit wave height.

Tests using irregular waves were not done because a means of coupling irregular wave kinematics between the models is not yet supported. The different test groups are summarized in Table II.

TABLE II
TEST CASES

Test Name	Wind	Waves (H,T)	Outcome
static F-D	aero off	still	mooring line force-disp.
LC14	aero off	still	platform transient resp.
LC41	aero off	6m, 10s	steady state response
LC51	8 m/s	6m, 10s	steady state response
LC54	8 m/s	2m, 1.8-63s	freq. resp. to waves

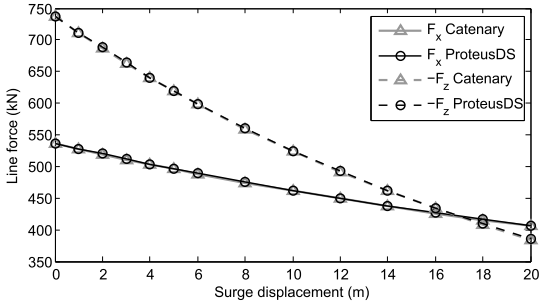

Fig. 2. Mooring line horizontal and vertical tensions at fairlead

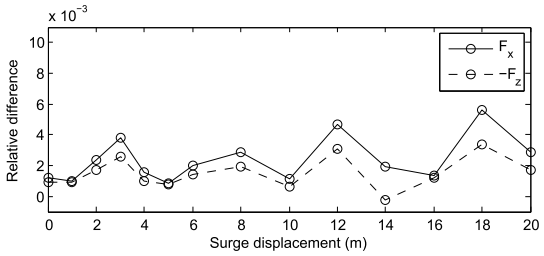

Fig. 3. Relative differences in fairlead tensions between Catenary and ProteusDS mooring models

III. RESULTS

A. Dynamic Model Verification

Tests were done using the dynamic ProteusDS mooring model under both static and dynamic conditions with varying levels of cable discretization. It was found that a cable discretized into 20 elements is suitable for the present work, having a fairlead force response agreeing with a 40-element discretization to within 0.2 percent, and being significantly faster to compute.

In the figures to follow, "'Catenary"' refers to results using FAST's default quasi-static mooring model, and "'ProteusDS"' refers to results using the dynamic FEM-based mooring model of that name. Comparison of the static equivalence of the two mooring models was done by using just the first mooring line from the Hywind design (along the positive x axis) and comparing the fairlead tensions once the line had come to static equilibrium with varying surge displacements of the platform. The comparison of the resulting forces in the x and z directions, for surge displacements going from 0 to 20 m in 2 m increments, is shown in Fig. 2. The corresponding relative differences between the two models are shown in Fig. 3. The static equivalence is very good, with percent errors staying below 0.6 percent. The spikes in the relative differences are likely caused by the discretization in the ProteusDS model from when a cable element transitions on or off the sea floor.

B. Load Case 1.4

The load case 1.4 tests are valuable in revealing the damping on the platform from platform hydrodynamics and mooring line dynamics. This is done by starting the platform in a

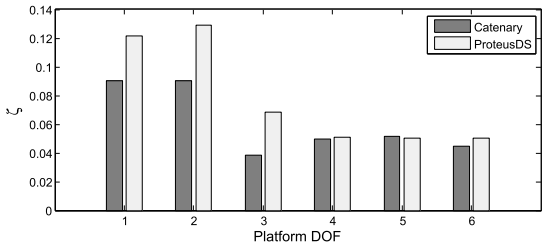

Fig. 4. Comparison of approximated damping coefficients for each platform DOF (1 - surge, 2 - sway, 3 - heave, 4 - roll, 5 - pitch, 6 -yaw)

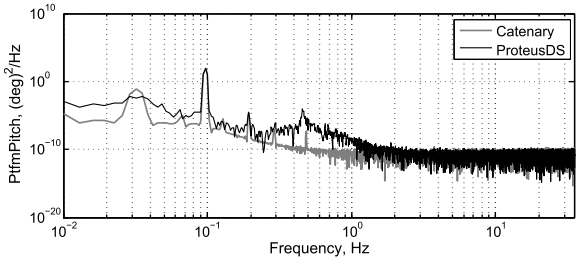

Fig. 5. PSD of platform pitch motions from LC 4.1

non-equilibrium position in still water and then observing its response as it comes to equilibrium. The decaying platform motion amplitudes were analyzed to extract the natural frequency and logarithmic decrement for the response of each DOF. From the averaged logarithmic decrement the equivalent linear damping on the platform can be approximated. The results for each DOF and for the quasi-static and the dynamic mooring models are given in Fig. 4.

The dynamic ProteusDS model clearly has the effect of increasing the damping on the platform in the translational DOFs. The effect on the rotational DOFs is much smaller, and in the case of the pitch DOF, the dynamic model shows a slightly reduced platform damping compared to the quasi-static model. The very small moment arms of the mooring lines on the platform are likely responsible for the minimal effect of the different mooring models on rotational DOF damping.

C. Load Case 4.1

The load case 4.1 tests allow comparison of the steady state response of the system without the effects of rotor aerodynamics. Fig. 5 shows the power spectral density of the platform's pitch DOF from both mooring models. It can be seen that both models have the same large amplitude of motions at F = 0.1 Hz corresponding to the 10 s period waves they are experiencing. The dynamic model results in increased excitation at adjacent frequencies, likely due to the additional nonlinear forces from mooring line dynamics, although the level of this excitation is small compared to the 0.1 Hz excitation.

D. Load Case 5.1

With the inclusion of aerodynamic forces, a fully coupled comparison is possible. Fig. 6 shows the power spectral density

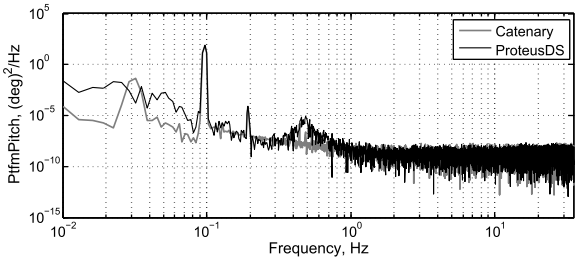

Fig. 6. PSD of platform pitch motions from LC 5.1

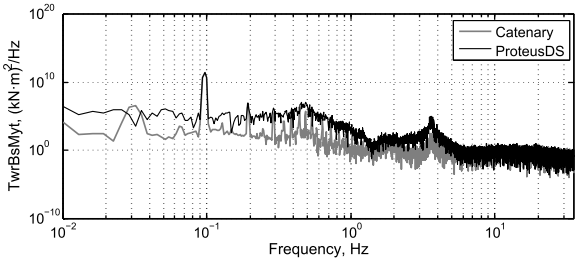

Fig. 7. PDS of tower base bending moment from LC 5.1

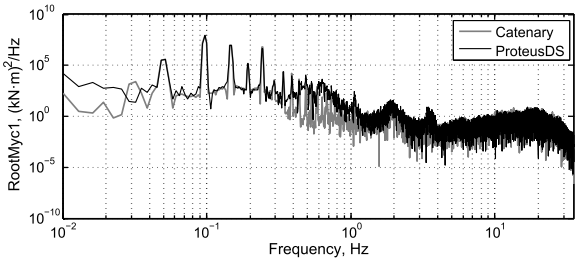

Fig. 8. PDS of blade root flapwise bending moment from LC 5.1

of the platform's pitch DOF. It is similar to the result from load case 4.1, but with reduced motions to either side of the 0.1 Hz spike. This is likely due to the damping effect of the wind turbine aerodynamics (when operating below rated power). The power spectral density plot of the tower base bending moment in the fore-aft direction, one of the critical loads for tower design, is shown in Fig. 7. It again has a large spike at 0.1 Hz corresponding to the wave excitation that agrees extremely closely between mooring models (1.6 percent higher in the quasi-static model). The dynamic mooring model provides a larger increase in the excitation at adjacent areas of the spectrum, however the power at these frequencies is still orders of magnitude less than the power at 0.1 Hz.

Fig. 8 shows the power spectral density plot of the blade root flapwise bending moment for one of the blades. This plot differs from the previous ones in that it shows several significant peaks at several different frequencies in addition to the dominant 0.1 Hz frequency. Under the steady 8 m/s winds of load case 5.1, the rotor rotates at approximately 9 RPM, or 0.15 Hz. The second-largest peak in Fig. 8 occurs at this frequency, suggesting the varying structural load on

the blade caused by changing conditions during it's rotation is significant, but not as significant as the structural loading caused by the wave-induced platform motions. The agreement between mooring models is within 1.5 percent for the 0.1 Hz peak, and within 1 percent for the 0.15 Hz peak. The agreement for the other large peaks is less good, on the order of 10 to 30 percent. The exact causes of these peaks and their disagreement are not clear, but they must originate from the different platform motions caused by the different mooring models.

Common between all of the power spectral density plots shown for both mooring models is a peak at 0.2 Hz, corresponding to double the wave frequency and likely a result of the phenomenon that some mooring line forces peak at both extremes of the platform motion cycle.

Figures 5, 6, and 7 all show a wide peak in the ProteusDS model results around 0.45 Hz. This frequency is the product of the rotor rotation frequency and the number of blades, and is a frequency at which structural loadings from the rotor aerodynamics often occur. However, the fact that this excitation is not noticeable in the Catenary mooring model results, and that it also appears in results from load case 4.1 (which has rotor rotation and aerodynamic forces disabled), suggests that this excitation in fact has nothing to do with the rotor but must be a direct result of the dynamic mooring model. The mooring phenomena that the ProteusDS model captures to cause this excitation is not clear from the current results.

E. Load Case 5.4

Load Case 5.4 considers the steady state response of the system from constant 8 m/s winds and regular waves of different frequencies. By normalizing the results by the incident wave height, effective response amplitude operators (RAOs) can be found for the various result channels of interest. The results from the two mooring models - in terms of platform surge, heave, and pitch, tower base bending moment, and blade root bending moments - are compared across wave frequencies of 0.1 to 3.5 Hz in 0.2 Hz increments. These are shown in Figures 9-14.

The agreement between the effective RAOs for the two mooring models is within 1 percent for regions of significant amplitude. The exception is the 0.1 Hz values for the pitch and tower bending moment RAOs, which disagree by 5 percent and 6 percent, respectively. It seems that the impact of including the mooring line dynamics becomes greater as the amplitude of the platform motion increases.

F. Discussion

The dynamic mooring model showed a large increase in the platform damping in the load case 1.4 tests, where the platform is moving in still water. However in situations where wave loading is the primary unsteady forcing on the system, the effect of the dynamic mooring model was minimal. A possible explanation is that in the first case, the moving platform and still water result in large relative water velocities over the cable elements, making a model that includes those hydrodynamic forces give different results than a model that ignores them. In the second case, where waves exist and are the driver of the platform oscillations, the platform motion and the wave motion act together, resulting in reduced relative water velocities over the cable elements, and a reduced importance of dynamic effects.

For the cables, the relative acceleration of the water is quite important, because the added mass coefficient is around 0.5. The impact of platform motion and wave velocities on relative water velocities over the cables both decrease with depth, because both the wave motion and the motion of the mooring line nodes resulting from the platform motion decrease with depth. The hypothesis presented suggests that tests with irregular wave conditions and/or fluctuating wind conditions, where the platform motions and wave motions will not always be of the same frequency and in phase, will give a more complete picture of the differences between using a quasi-static and a dynamic mooring model in general floating wind turbine simulations.

IV. Conclusions

The dynamic FEM-based mooring model ProteusDS was coupled to floating wind turbine simulator FAST to provide a means of comparing quasi-static and dynamic mooring models. The static equivalence of the dynamic model and FAST's built-in quasi-static mooring model is very good. Tests using both models were performed looking at scenarios of platform transient unforced response and the coupled system response to regular waves and steady winds. The dynamic mooring model significantly increased the overall platform damping in translational DOFs during motion decay tests in still water. There was very little difference between the models in coupled tests where wave excitation is the primary driver of platform motions, except for the addition of small levels of higher frequency system responses from the dynamic model.

One would expect platform damping to be important to the system response when excited by waves. The nature of the different tests suggests that it is only in situations where the platform motions and wave velocities are not synchronized that the damping from the dynamic mooring model will make a large difference. Tests using irregular waves will be the best way to explore this hypothesis.

V. Future work

Simulations with irregular waves will enable the exploration of two phenomena not examined in the present study - the impact of the mooring model on turbine structure fatigue, and the effect of the dynamic mooring model when experiencing motion and water velocities of multiple frequencies. It is expected that the coupling capabilities for irregular sea states in the interface between ProteusDS and FAST will be developed soon.

Future comparisons should expand the scope to look at different floating wind turbine designs from different stability classes and test at various depths. This will provide a broader

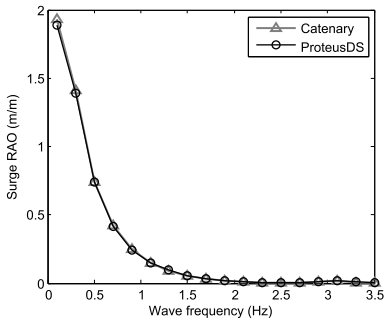

Fig. 9. Surge RAO

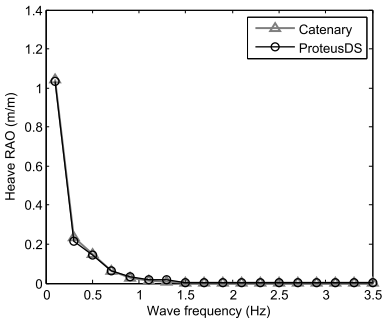

Fig. 10. Heave RAO

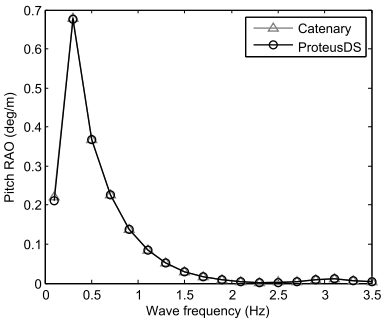

Fig. 11. Pitch RAO

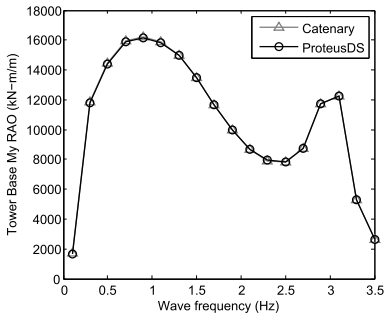

Fig. 12. Tower bending moment RAO

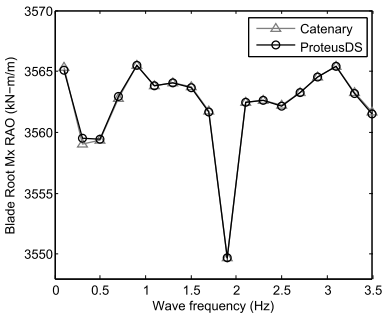

Fig. 13. Blade root flapwise bending moment RAO

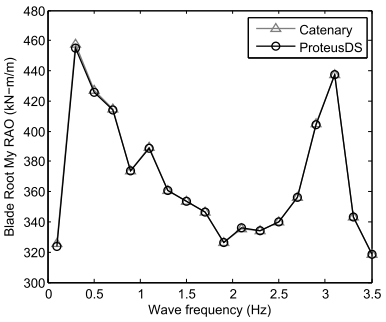

Fig. 14. Blade root spanwise bending moment RAO

understanding of the importance of mooring line dynamics for different floating wind turbine simulations.

REFERENCES

[1] W. Musial and S. Butterfield, "Future for offshore wind energy in the united states," National Renewable Energy Laboratory, Golden, Colorado, Tech. Rep. 36313, Jun. 2004.

[2] A. Cordle, "State of the art design tools for floating offshore wind turbines," Project UpWind, Tech. Rep., Mar. 2010.

[3] J. M. Jonkman, "Dynamics modeling and loads analysis of an offshore floating wind turbine," National Renewable Energy Laboratory, Golden, Colorado, Tech. Rep. 41958, Nov. 2007.

[4] M. B. Waris and T. Ishihara, "Influence of mooring force estimation on dynamic response of floating offshore wind turbine system," in *Renewable Energy 2010 International Conference*, Yokohama, Japan, 2010.

[5] B. S. Kallesoe, U. S. Paulsen, A. Kohler, and H. F. Hansen, "Aero-Hydro-Elastic response of a floating platform supporting several wind turbines," in *49th AIAA Aerospace Sciences Meeting*, Orlando, Florida, Jan. 2011.

[6] B. J. Buckham, F. R. Driscoll, M. Nahon, and B. Radanovic, "Torsional mechanics in dynamics simulation of low-tension marine tethers," *International Journal of Offshore and Polar Engineering*, vol. 14, no. 3, pp. 218–226, 2003.

[7] M. Berzeri and A. A. Shabana, "Development of simple models for the elastic forces in the absolute nodal co-ordinate formulation," *Journal of Sound and Vibration*, vol. 235, no. 4, pp. 539–565, Aug. 2000.

[8] J. M. Jonkman and et al., "Offshore code comparison collaboration with IEA wind task 23: Phase IV results regarding floating wind turbine modelling," National Renewable Energy Laboratory, Golden, Colorado, Tech. Rep. 47534, Apr. 2010.

[9] J. M. Jonkman, "Definition of the floating system for phase IV of OC3," National Renewable Energy Laboratory, Golden, Colorado, Tech. Rep. 47535, May 2010.